Evaluated ^{55}Mn and ^{90}Zr covariances in fast neutron region

M.T. Pigni, M. Herman, P. Obložinský

National Nuclear Data Center,
Brookhaven National Laboratory, Upton, NY 11973-5000, U.S.A.
pigni@bnl.gov

1. Introduction

We have completed new covariance evaluations for ^{55}Mn and ^{90}Zr covering incident neutron energies from keV range to 20 MeV. Evaluations for these two important structural materials are motivated by the needs of nuclear criticality safety applications and the GNEP data adjustment project. We consider the most important neutron-induced reaction channels: total, inelastic scattering, capture, and (n,2n).

2. Methodology

The methodology combines the nuclear model predictions with experimental data. The nuclear reaction model code EMPIRE was used to calculate sensitivity to model parameters. This was done by perturbation of parameters that define the optical model potential, nuclear level densities and strength of the pre-equilibrium emission. The sensitivity analysis was performed with the set of parameters which reproduces as much as possible the ENDF/B-VII.0 cross sections. This choice was motivated by the necessity of retaining validated ENDF/B-VII.0 evaluations. The experimental data were analyzed and both statistical and systematical uncertainties were extracted for selected experiments. Then, the Bayesian code KALMAN and/or (generalized) least square procedures were used to combine the sensitivity analysis (*a priori* information) and the experiments to obtain the evaluated covariance matrices (*a posteriori* information).

3. Bayesian algorithm

The KALMAN code is used as a nuclear data evaluation tool based on the iterative generalized least-squares approach. The procedure emphasizes the estimation of the uncertainties in the model parameters, and the corresponding correlations. It is applied to evaluating neutron cross sections and their covariance matrices for various reaction channels. Applying the Bayesian equations is straightforward, and the update is a simple algebraic operation,

$$\mathbf{x}' = \mathbf{x} + \mathbf{X}\hat{\mathbf{S}}^{\mathrm{T}}(\hat{\mathbf{S}}\mathbf{X}\hat{\mathbf{S}}^{\mathrm{T}} + \mathbf{V})^{-1}(\boldsymbol{\eta} - \boldsymbol{\sigma}(\mathbf{x}))$$

$$\mathbf{X}' = \mathbf{X} - \mathbf{X}\hat{\mathbf{S}}^{\mathrm{T}}(\hat{\mathbf{S}}\mathbf{X}\hat{\mathbf{S}}^{\mathrm{T}} + \mathbf{V})^{-1}\hat{\mathbf{S}}\mathbf{X} \qquad (1)$$

- $\mathbf{X} \equiv \langle \delta x_\ell \, \delta x_m \rangle$ covariance matrix of the model parameters.
- $\hat{\mathbf{S}}^{\mathrm{T}} = \mathbf{S}^{\mathrm{T}}(\hat{\mathbf{x}})$ transpose sensitivity matrix where $\hat{\mathbf{x}}$ satisfies the least-square condition. Sensitivity matrices are generally rectangular with elements $S_{i,j} = \frac{\partial \sigma(E_i, \hat{\mathbf{x}})}{\partial x_j}$.
- $\mathbf{V} \equiv \langle \delta\eta_k \, \delta\eta_\mu \rangle$ covariance matrix of experimental cross sections, $\boldsymbol{\eta} = \{\eta_1, \ldots, \eta_k, \ldots, \eta_\mu, \ldots\}$.
- $\boldsymbol{\sigma}(\mathbf{x})$ vector of cross sections for a specific reaction channel calculated for the set of parameter $\mathbf{x}$.

4. Model parameter

Table 1: Optical-model parameter uncertainties (in %) used for the *prior*: r - radius, a - diffuseness, V - real depth, W - imaginary depth. The subscripts, v, s, and w, respectively, denote real volume, real surface, and imaginary surface. The superscripts, $tg \equiv$ n + $\frac{A}{Z}$ and $np \equiv$ p + $\frac{A+1}{Z-1}$, refer to nucleon-nucleus interaction.

Δr_s^{tg}	Δr_v^{tg}	Δr_w^{tg}	ΔV_v^{tg}	ΔW_s^{tg}	ΔW_v^{tg}	Δa_s^{tg}	Δa_v^{tg}	ΔV_v^{np}	ΔW_s^{np}
3-5	5	5	5	3-5	5	5	5	5	5

Table 2: Parameter uncertainties (in %) used for the Hauser-Feshbach, exciton models, and deformation (Def): $\tilde{a}$ - total level density, $\tilde{g}$ - single-particle level density, f_γ - gamma-ray strength functions, and mfp - nucleon mean-free path. The superscripts refer to $cn \equiv$ compound, $tg \equiv$ target, $n2n \equiv$ (n,2n) residue, $np \equiv$ (n,p) residue.

$\Delta\tilde{a}^{cn}$	$\Delta\tilde{a}^{tg}$	$\Delta\tilde{a}^{n2n}$	$\Delta\tilde{a}^{np}$	$\Delta\tilde{g}^{np}$	$\Delta\tilde{g}^{tg}$	Δf_γ	Δmfp	ΔDef
15	15	15	15	15	15	10-15	25	35

5. Experiments

Table 3: Sets of experimental data used in the covariance evaluation of ^{55}Mn and ^{90}Zr.

Reaction / Nucleus	(n,tot)	(n,n′)	(n,2n)	(n,γ)
^{55}Mn	1	3	12	4
^{90}Zr	2	0	4	1

6. Results - ^{55}Mn

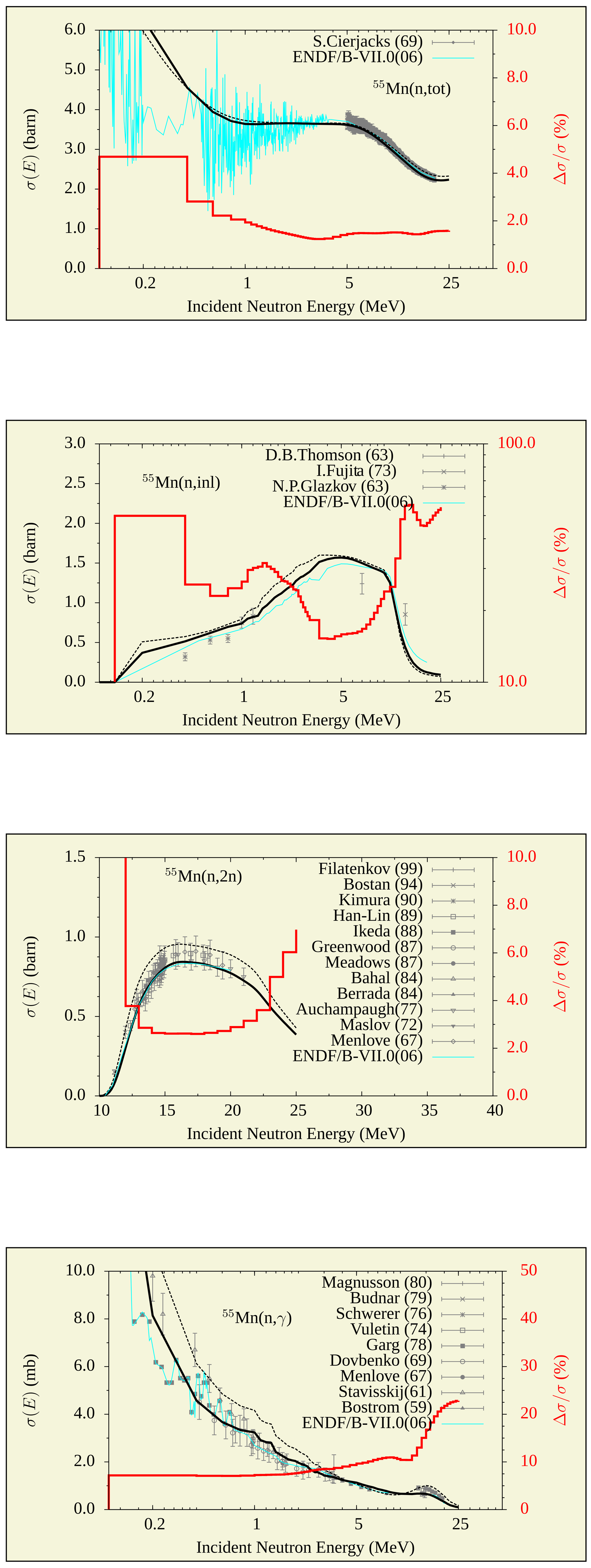

Figure 1: Dashed and continuous black lines refer to the *prior* and *posterior* cross sections, respectively. Also shown (in red) are relative uncertainties. From top to bottom: Total, inelastic, (n,2n), and (n,γ) reaction channels.

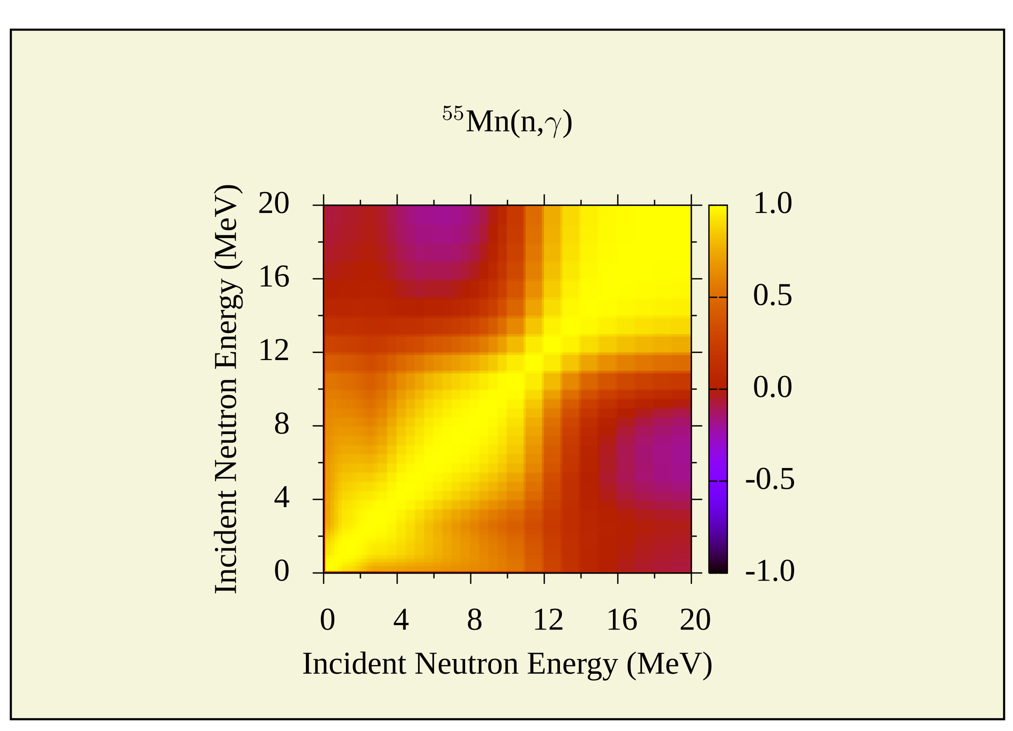

Figure 2: Correlation matrix for the (n,γ) reaction channel.

7. Results - ^{90}Zr

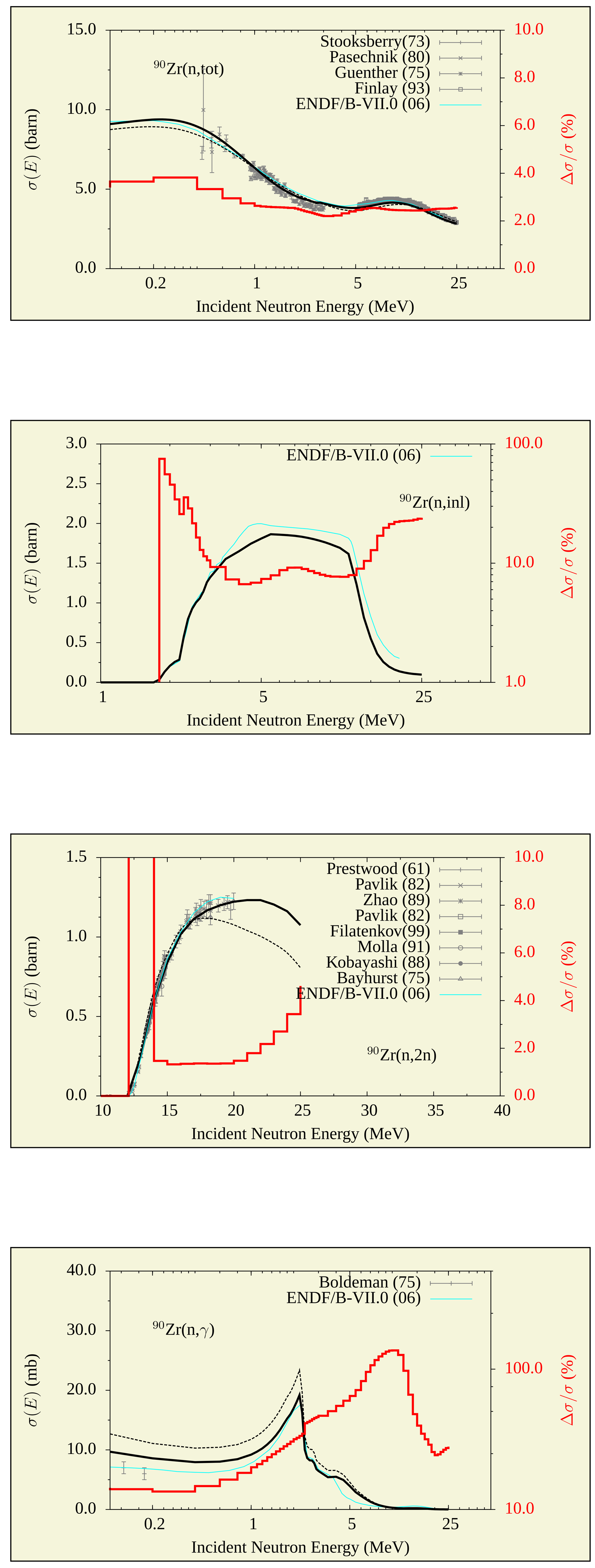

Figure 3: Dashed and continuous black lines refer to the *prior* and *posterior* cross sections, respectively. Also shown (in red) are relative uncertainties. From top to bottom: Total, inelastic, (n,2n), and (n,γ) reaction channels.

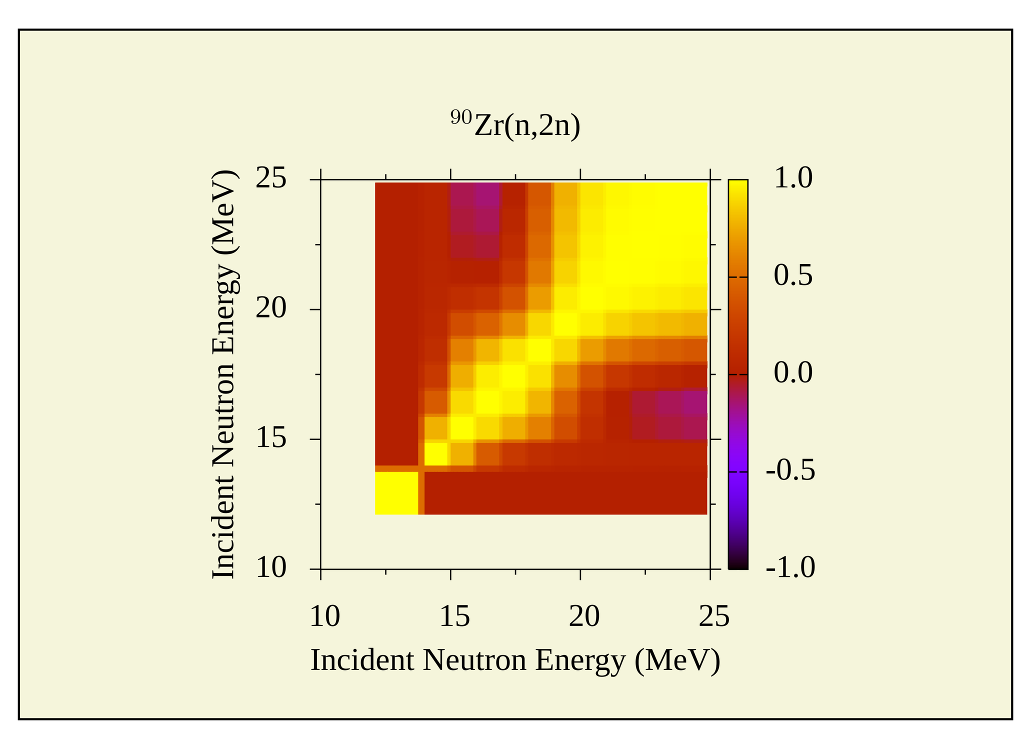

Figure 4: Correlation matrix for the (n,2n) reaction channel.

Sponsored by the Office of Nuclear Physics - Office of Science - U.S. Department of Energy